mathematics

MDPI

Article

Stability Analysis of the Rational Solutions, Periodic Cross-Rational Solutions, Rational Kink Cross-Solutions, and Homoclinic Breather Solutions to the KdV Dynamical Equation with Constant Coefficients and Their Applications

Aly R. Seadawy [1,*], Syed T. R. Rizvi [2] and Hanadi Zahed [1]

[1] Mathematics Department, Faculty of Science, Taibah University, Al-Madinah Al-Munawarah 41411, Saudi Arabia
[2] Department of Mathematics, COMSATS University Islamabad, Lahore Campus, Punjab 54000, Pakistan
* Correspondence: aabdelalim@taibahu.edu.sa

Abstract: We explore various analytical rational solutions with symbolic computation using the ansatz transformation functions. We gain a variety of rational solutions such as *M*-shaped rational solutions (MSRs), periodic cross-rationals (PCRs), multi-wave solutions, rational kink cross-solutions (RKCs), and homoclinic breather solutions (HBs), and by using the appropriate values for the relevant parameters, their dynamics are visualized in figures. Additionally, two different types of interactions between MSRs and kink waves are analyzed. Furthermore, we examine the stability of the obtained solutions and create a corresponding table. We analyze the stability of these solutions and the movement role of the wave by making graphs as two-dimensional, three-dimensional and density graphs as well as contour visual and stream plots.

Keywords: exact solutions; periodic cross-rational; *M*-shaped rational solutions; breather solitons; KdV equation

MSC: 35J05; 35J10; 35K05; 35L05

Citation: Seadawy, A.R.; Rizvi, S.T.R.; Zahed, H. Stability Analysis of the Rational Solutions, Periodic Cross-Rational Solutions, Rational Kink Cross-Solutions, and Homoclinic Breather Solutions to the KdV Dynamical Equation with Constant Coefficients and Their Applications. *Mathematics* **2023**, *11*, 1074. https://doi.org/10.3390/math11051074

Academic Editor: Ioannis K. Argyros

Received: 4 January 2023
Revised: 30 January 2023
Accepted: 16 February 2023
Published: 21 February 2023

1. Introduction

A partial differential equation (PDE) depicts the relationships between several partial derivatives of a variety of multivariate functions. Physics and engineering are two mathematics-based sciences that frequently use PDEs [1–4]. The fundamentals of contemporary scientific logic are formed by them for several ideas, including heat, sound, diffusion, electrodynamics [5–7], electrostatics, elastic, hydrodynamics, and quantum mechanics [8–10]. A wide range of scientific fields are interested in studying nonlinear wave phenomena [11–14]. This has to do with comprehending actual water waves, the way light interacts with matter, how optical fibers transmit light, how traffic moves, how earthquakes happen, and how galaxies grow. Nonlinear wave theory is a recent mathematical field that commonly investigates asymptotic regimes (including fluctuating over several scales, high frequencies, or large amplitudes) that are difficult to approach through numerical simulations [15–19].

The (2+1)-dimensional KdV equation was taken into consideration in this work. For nonlinear partial differential equation (NLPDE) solutions, several techniques have been used in the literature. The pursuit of accurate NLPDE solutions is crucial for comprehending nonlinear physical phenomena [20–26]. For instance, kink-shaped tanh solutions and bell-shaped sech solutions are frequently used to simulate the nonlinear wave phenomena that are observed in optical fibers, fluid dynamics, and plasma [27–31]. Numerous authors who have an interest in nonlinear physical phenomena have recently looked at the exact solutions of NLPDEs. These authors have provided a large number of effective techniques

for the instance inverse scattering technique [32], Darboux transform [33], F-expansion scheme [34], generalized Riccati equation [35], Painleve expansion technique [36], Backlund transform [37], exp-function expansion mechanism [38], extended tanh function approach [39,40], and (G'/G)-expansion method [41].

The KdV equation with constant coefficients in the (2+1)-dimensional space is given by [42]

$$\Gamma_{ty} + \Gamma_{xxxy} + \delta\Gamma_{yx}\Gamma_x + \delta\Gamma_y\Gamma_{xx} + \eta\Gamma_{xx} + \lambda\Gamma_{yy} = 0, \tag{1}$$

$$\Gamma(x, y, t) = \Lambda(\varepsilon), \quad \varepsilon = x - \rho y - ct. \tag{2}$$

By utilizing the above transformation in Equation (1), we obtain

$$\rho c\Lambda'' - \rho\Lambda'''' - 2\delta\rho\Lambda'\Lambda'' + \eta\Lambda'' + \lambda\rho^2\Lambda'' = 0, \tag{3}$$

If the equation is integrated once into the final scenario, then the following equation is produced:

$$(\rho c + \eta + \lambda\rho^2)\Lambda' - \delta\rho(\Lambda')^2 - \rho\Lambda''' = 0. \tag{4}$$

Numerous researchers have worked on the governing model. For instance, Wazwaz et al. examined the Painleve test to look at the conditions for compatibility in order to make sure that the suggested model could be integrated [42]. Ma obtained N-soliton solutions for the (2+1)-dimensional KdV equation, the Kadomtsev–Petviashvili equation, and the (2+1)-dimensional Hirota–Satsuma–Ito equation by analyzing the Hirota N-soliton conditions [43]. Ma et al. presented the diversity of interaction solutions to the (2+1)-dimensional Ito equation, such as the combined multi-wave solutions which were analyzed in [44]. Zayed et al. investigated a two-variable $(\frac{G'}{G}, \frac{1}{G})$ expansion technique for the nonlinear KdV equation [45]. By using the symbolic computation with various ansatz transformations for Equation (1), this manuscript aims to evaluate MSR and their interactions with one and two kink waves, PCRs, RKCs, multi-wave solutions, and HBs.

This article is set up as follows. In Section 2, we assess the MSRs and examine their associated 3D visualizations. Section 3 provides a concise analysis of the interaction of MSRs with a single exponential function along several 3D, 2D, and contour profiles. In Section 4, we calculate the interaction solution of M-shaped double exponential functions for the provided model using the necessary 3D, 2D, and contour plots. Section 5 evaluates RKCs and their findings for various parameters. In Section 6, we will discuss PCRs, and we will draw some associated graphs. In Section 7, we will explore multi-wave solutions and make graphical visuals with suitable parameters. In Section 8, we will study the interactional solution of MSRs with a rogue wave solution. HBs and their pictorial representations are dispatched in Section 9. The stability property of the solutions is covered in Section 10, along with how it applies to all solutions that were found. In Section 11, we discuss our findings and debate them. Finally, in Section 12, we make our final observations.

2. Rational *M*-Shaped Solution (MSRs)

Let us use the transformation [46]

$$\Lambda(\varepsilon) = 2(ln\omega)_\varepsilon, \tag{5}$$

If this transformation is substituted into Equation (5), hten the bilinear form shown below is obtained:

$$\begin{aligned} &-2\eta\omega^2\omega'^2 - 2c\rho\omega^2\omega'^2 - 2\lambda\rho^2\omega^2\omega'^2 + 12\rho^4 - 4\delta\rho\omega'^4 + 2\eta\omega^3\omega'' + 2c\rho\omega^3\omega'' + 2\lambda\rho^2\omega^3\omega'' - \\ &24\rho\omega\omega'^2\omega'' + 8\delta\rho\omega\omega'^2 + 6\rho\omega^2\omega''^2 - 4\delta\rho\omega^2\omega''^2 + 8\rho\omega^2\omega'\omega'' - 2\rho\omega^3\omega'''' = 0. \end{aligned} \tag{6}$$

Now, we use this bilinear form to evaluate various rational and interactional solutions. For MSRs, we consider $'\omega'$ as [47]

$$\omega = \varepsilon_1^2 + \varepsilon_2^2 + m_5, \tag{7}$$

where

$$\varepsilon_1 = m_1\varepsilon + m_2, \;\; \varepsilon_2 = m_3\varepsilon + m_4.$$

However, $m_j (1 \leq j \leq 5)$ represents any constants. By using Equation (7) in Equation (6) and collecting the coefficients of ε, we then solve the system of equations to find the values of the parameters:

$$\delta = \tfrac{-13}{2}, \; m_1 = -1, \; m_3 = m_2 = 0, m_5 = \tfrac{-(\lambda\rho^2 m_4^2 + \rho m_4^2 c + \eta m_4^2 - 36\rho)}{\lambda\rho^2 + \rho c\eta}. \tag{8}$$

Via the above parametric values, we have

$$\omega = m_4^2 + \varepsilon^2 + \frac{(-m_4^2\eta + 36\rho - m_4^2 c\rho - m_4^2\lambda)}{\eta + c\rho + \lambda\rho^2}. \tag{9}$$

By using Equation (9) in Equation (5), we obtain

$$\Lambda(\varepsilon) = \frac{4\varepsilon}{m_4^2 + \varepsilon^2 + \frac{(-m_4^2\eta + 36\rho - m_4^2 c\rho - \lambda\rho^2)}{\eta + c\rho + \lambda\rho^2}}. \tag{10}$$

By replacing Equation (2) with Equation (10), we obtain the M-shape rational solution of Equation (1):

$$\Gamma_1(x, y, t) = \frac{4(-ct + x - y\rho)}{m_4^2 + (-ct + x - y\rho)^2 + \frac{(-m_4^2\eta + 36\rho - m_4^2 c\rho - \lambda\rho^2)}{\eta + c\rho + \lambda\rho^2}}. \tag{11}$$

Equation (11) specifies the MSRs, and $\Gamma(x, y, t)$ is graphed with $\eta = -1, \; c = 2, \rho = 2$, $\lambda = 2$, and $m_4 = 9$.

3. MSR with a One-Kink Solution

In this section, we explore MSRs with kink rational solutions using the following transformation [48]

$$\omega = \kappa_1^2 + \kappa_2^2 + z_1\kappa_3, \tag{12}$$

where

$$\kappa_1 = g_1\varepsilon + g_2, \;\; \kappa_2 = g_3\varepsilon + g_4, \;\; \kappa_3 = g_5\varepsilon + g_6.$$

However, $g_j (1 \leq j \leq 6)$, where all are assumed to be parameters. By inserting Equation (12) into Equation (6), and by using mathematica, we can evaluate all the coefficients ε. We obtain equations which provide the following values:

$$g_2 = \tfrac{-1}{2} g_1 \tfrac{(4\delta + 11)}{\delta\sqrt{\frac{-(-\lambda\rho^2 - \rho c - \eta)}{\delta}}}, \; g_5 = \sqrt{\tfrac{-(-\lambda\rho^2 - \rho c - \eta)}{\delta}}, \; g_3 = 0. \tag{13}$$

By utilizing the above values, we obtain

$$\omega = g_4^2 + e^{g_6 + \varepsilon\sqrt{c + \frac{\eta}{\rho} + \lambda\rho}} z_1 + \left(g_1\varepsilon - \frac{g_1(11 + 4\delta)}{2\delta\sqrt{c + \frac{\eta}{\rho} + \lambda\rho}} \right). \tag{14}$$

Inserting Equation (14) into Equation (5) yields

$$\Lambda(\varepsilon) = \frac{2\left(e^{g_6+\varepsilon\sqrt{c+\frac{\eta}{\rho}+\lambda\rho}}z_1\sqrt{c+\frac{\eta}{\rho}+\rho}+2g_1\left(g_1\varepsilon-\frac{g_1(11+4\delta)}{2\delta\sqrt{c+\frac{\eta}{\rho}+\lambda\rho}}\right)\right)}{g_4^2+e^{g_6+\varepsilon\sqrt{c+\frac{\eta}{\rho}+\lambda\rho}}z_1+\left(g_1\varepsilon-\frac{g_1(11+4\delta)}{2\delta\sqrt{c+\frac{\eta}{\rho}+\lambda\rho}}\right)}. \tag{15}$$

By substituting Equation (15) into Equation (2), we achieve the MSR with a one-kink solution for Equation (1):

$$\Gamma_2(x,y,t) = \frac{2\left(e^{g_6+(-ct+x-y\rho)\sqrt{c+\frac{\eta}{\rho}+\lambda\rho}}z_1\sqrt{c+\frac{\eta}{\rho}+\rho}+2g_1\left(g_1(-ct+x-y\rho)-\frac{g_1(11+4\delta)}{2\delta\sqrt{c+\frac{\eta}{\rho}+\lambda\rho}}\right)\right)}{g_4^2+e^{g_6+(-ct+x-y\rho)\sqrt{c+\frac{\eta}{\rho}+\lambda\rho}}z_1+\left(g_1(-ct+x-y\rho)-\frac{g_1(11+4\delta)}{2\delta\sqrt{c+\frac{\eta}{\rho}+\lambda\rho}}\right)}. \tag{16}$$

4. MSR with a Two-Kink Solution

In this section, we work on MSRs with double kinks which consist of two exponential functions. We consider [2]

$$\omega = \zeta_1^2+\zeta_2^2+z_1e^{\zeta_3}+z_2e^{-\zeta_4}, \tag{17}$$

where

$$\zeta_1 = u_1\varepsilon+u_2,\ \ \zeta_2 = u_3\varepsilon+u_4,\ \ \zeta_3 = u_5\varepsilon+u_6,\ \ \zeta_4 = u_7\varepsilon+u_8.$$

However, $u_j(1\le j\le 8)$ are all constants. We put Equation (17) into Equation (6) using mathematica and calculated the coefficients of ε and the exponential functions. We obtain a system of equations that provides the values of the constants:

$$u_1 = \tfrac{1}{5}\sqrt{2}\sqrt{5},\ u_7 = \sqrt{\tfrac{-1}{2}\tfrac{(\lambda\rho^2+\rho c+\eta)}{\rho}},\ u_2 = \tfrac{-8}{5}\frac{(\delta+2)\sqrt{2}\sqrt{5}}{(4\delta+3)\sqrt{\tfrac{-1}{2}\tfrac{(\rho^2+\rho c+\eta)}{\rho}}}, \tag{18}$$

$$u_4 = \frac{\sqrt{\frac{-(-624\delta^2\rho-3336\delta\rho-3651\rho)}{20\lambda\rho^2+20\rho c+20\eta}}}{(4\delta+3)},\ u_8 = u_3 = 0,\ u_5 = \sqrt{\frac{(-\rho\rho^2-\rho c-\eta)}{2\rho}}.$$

Using the obtained values in Equation (17), we obtain

$$\omega = e^{u_6+\frac{\varepsilon\sqrt{\frac{-\eta+c\rho+\rho^3}{\rho}}}{\sqrt{2}}}z_1+e^{-u_8-\frac{\varepsilon\sqrt{\frac{-\eta+\rho(c+\lambda\rho)}{\rho}}}{\sqrt{2}}}z_2+\left(u_3\varepsilon+\frac{2\sqrt{\frac{3}{5}}\sqrt{\frac{(1217+1112\delta+208\delta^2)\rho}{\eta+\rho(c+\lambda\rho)}}}{(3+4\delta)}\right)^2 \tag{19}$$
$$+\left(\sqrt{\tfrac{2}{5}}\varepsilon-\frac{16(2+\delta)}{\sqrt{5}(3+4\delta)\sqrt{\frac{-\eta+\rho(c+\lambda\rho)}{\rho}}}\right)^2.$$

Inserting Equation (19) into Equation (5) gives

$$\Lambda(\varepsilon) = \frac{2\left(\frac{4}{5}\varepsilon+\frac{e^{u_6+\frac{\varepsilon\vartheta}{\sqrt{2}}}z_1\vartheta}{\sqrt{2}}-\frac{6\sqrt{2}(2+\delta)}{5(3+4\delta)\vartheta}-\frac{e^{-u_8-\frac{\varepsilon\vartheta}{\sqrt{2}}}z_2\vartheta}{\sqrt{2}}+2u_3\mu\right)}{e^{u_6+\frac{\varepsilon\vartheta}{\sqrt{2}}}z_1+e^{-u_8-\frac{\varepsilon\vartheta}{\sqrt{2}}}z_2+\left(u_3\varepsilon+\frac{2\sqrt{\frac{3}{5}}\sqrt{\frac{(1217+1112\delta+208\delta^2)\rho}{\eta+\rho(c+\lambda\rho)}}}{(3+4\delta)}\right)^2+\left(\sqrt{\frac{2}{5}}\varepsilon-\frac{16(2+\delta)}{\sqrt{5}(3+4\delta)\vartheta}\right)^2}, \tag{20}$$

where

$$\mu = \left(u_3\varepsilon+\frac{2\sqrt{\frac{3}{5}}\sqrt{\frac{(1217+1112\delta+208\delta^2)\rho}{\eta+\rho(c+\lambda\rho)}}}{(3+4\delta)}\right),\ \vartheta = \sqrt{\frac{-\eta+c\rho+\rho^3}{\rho}}.$$

Inserting Equation (20) into Equation (2) gives the MSR with a double-kink solution to Equation (1):

$$\Gamma_3(x,y,t)=\frac{2\left(-\frac{4}{5}(ct-x+y\rho)+\frac{e^{u_6+\frac{(ct-x+y\rho)\vartheta}{\sqrt{2}}}z_1\vartheta}{\sqrt{2}}-\frac{6\sqrt{2}(2+\delta)}{5(3+4\delta)\vartheta}-\frac{e^{-u_8-\frac{(ct-x+y\rho)\vartheta}{\sqrt{2}}}z_2\vartheta}{\sqrt{2}}+2u_3\mu\right)}{e^{u_6+\frac{(ct-x+y\rho)\vartheta}{\sqrt{2}}}z_1+e^{-u_8-\frac{(ct-x+y\rho)\vartheta}{\sqrt{2}}}z_2+\nu^2+\left(\sqrt{\frac{2}{5}}(ct-x+y\rho)-\frac{16(2+\delta)}{\sqrt{5}(3+4\delta)\vartheta}\right)^2} \tag{21}$$

where

$$\nu=\left(u_3(ct-x+y\rho)+\frac{2\sqrt{\frac{3}{5}}\sqrt{\frac{(1217+1112\delta+208\delta^2)\rho}{\eta+\rho(c+\lambda\rho)}}}{(3+4\delta)}\right),\ \vartheta=\sqrt{\frac{-\eta+c\rho+\rho^3}{\rho}},$$

$$\mu=\left(u_3\varepsilon+\frac{2\sqrt{\frac{3}{5}}\sqrt{\frac{(1217+1112\delta+208\delta^2)\rho}{\eta+\rho(c+\lambda\rho)}}}{(3+4\delta)}\right).$$

5. Rational Kink Cross Solution (RKCs)

We use the transformation [1]

$$\omega=e^{-\sigma_1}+m_0e^{\sigma_1}+\sigma_2^2+\sigma_3^2+q_7, \tag{22}$$

where

$$\sigma_1=q_1\varepsilon+q_2,\ \ \sigma_2=q_3\varepsilon+q_4,\ \ \sigma_3=q_5\varepsilon+q_6.$$

However, $g_j(1\le j\le 5)$ are all real-valued constants. We insert Equation (22) into Equation (6) and compute all the coefficients of the exponential functions and powers of ε. We gain equations which provide the following values:

$$m_4=0,\ \delta=\tfrac{-9}{4},\ q_1=\sqrt{\tfrac{-1}{9}\tfrac{(2\lambda\rho^2+2\rho c+2\eta)}{\delta}},\ q_6=\frac{2(q_3^2+q_5^2)}{\sqrt{\frac{-1}{9}\frac{(2\lambda\rho^2+2\rho c+2\eta)q_5}{\delta}}}. \tag{23}$$

We then use Equation (23) in Equation (22):

$$\omega=q_7+e^{-q_2-\frac{1}{3}\sqrt{2}\varepsilon\sqrt{\frac{-\eta+\rho(c+\lambda\rho)}{\rho}}}+e^{q_2+\frac{1}{3}\sqrt{2}\varepsilon\sqrt{\frac{-\eta+\rho(c+\lambda\rho)}{\rho}}}m_0+q_3^2\varepsilon^2+(q_5\varepsilon+\frac{3\sqrt{2}(q_3^2+q_5^2)}{q_5\sqrt{\frac{-\eta+\rho(c+\lambda\rho)}{\rho}}})^2. \tag{24}$$

By substituting Equation (24) into Equation (5), we obtain

$$\Lambda(\varepsilon)=\frac{\left(2\left(2q_3^2\varepsilon+2q_5^2\varepsilon+\frac{6\sqrt{2}(q_3^2+q_5^2)}{\varphi}-\frac{1}{3}\sqrt{2}\tau\varphi+\frac{1}{3}\sqrt{2}e^{q_2+\frac{1}{3}\sqrt{2}\varepsilon\varphi}m_0\varphi\right)\right)}{q_7+\tau+e^{q_2+\frac{1}{3}\sqrt{2}\varepsilon\varphi}m_0+q_3^2\varepsilon^2+(q_5\varepsilon+\frac{3\sqrt{2}(q_3^2+q_5^2)}{q_5\varphi})^2}, \tag{25}$$

where

$$\tau=e^{-q_2-\frac{1}{3}\sqrt{2}\varepsilon\sqrt{\frac{-\eta+\rho(c+\lambda\rho)}{\rho}}},\ \varphi=\sqrt{\frac{-\eta+\rho(c+\lambda\rho)}{\rho}}.$$

We then substitute Equation (25) into Equation (2) to find the RKCs of Equation (1):

$$\Gamma_4(x,y,t) = \left(2\left(2q_3^2(ct-x+\rho y)+2q_5^2(ct-x+\rho y)+\frac{6\sqrt{2}(q_3^2+q_5^2)}{\varphi}-\frac{1}{3}\sqrt{2}\tau\varphi+\frac{1}{3}\sqrt{2}\right.\right. \quad (26)$$
$$\left.\left.e^{q_2+\frac{1}{3}\sqrt{2}(ct-x+\rho y)\varphi}m_0\varphi\right)\right)/q_7+\tau+e^{q_2+\frac{1}{3}\sqrt{2}(ct-x+\rho y)\varphi}m_0+q_3^2(ct-x+\rho y)^2+$$
$$(q_5(ct-x+\rho y)+\frac{3\sqrt{2}(q_3^2+q_5^2)}{q_5\varphi})^2.$$

where

$$\tau = e^{-q_2-\frac{1}{3}\sqrt{2}\varepsilon\sqrt{\frac{-\eta+\rho(c+\lambda\rho)}{\rho}}},\ \varphi = \sqrt{\frac{-\eta+\rho(c+\lambda\rho)}{\rho}}.$$

6. Periodic Cross-Rational Solutions (PCRs)

We use the transformation [49]

$$\omega = \varpi_1^2+\varpi_2^2+m_1\cos(\varpi_3)+m_2\cosh(\varpi_4)+e_9, \quad (27)$$

where

$$\varpi_1 = e_1\varepsilon+e_2,\ \ \varpi_2 = e_3\varepsilon+e_4,\ \ \varpi_3 = e_5\varepsilon+e_6,\ \ \varpi_4 = e_7\varepsilon+e_8.$$

However, $e_j(1 \le j \le 9)$ are all real-valued parameters. We put Equation (27) into Equation (6) and collect equations by comparing the coefficients of the trigonometric function to obtain

$$\delta = \frac{15}{8},\ e_1 = Ie_3,\ e_5 = \sqrt{\frac{-1}{3}\frac{(2\lambda\rho^2+2\rho c+2\eta)}{\rho}},\ e_7 = \sqrt{\frac{-1}{3}\frac{(-2\lambda\rho^2-2\rho c-2\eta)}{\rho}}. \quad (28)$$

By putting Equation (28) into Equation (27), we obtain

$$\omega = e_9+(e_2+ie_3)^2+(e_4+e_3\varepsilon)^2+m_1\cos\left(e_6+\frac{\varepsilon\sqrt{\frac{-2\eta+2c\rho+2\lambda\rho^2}{\rho}}}{\sqrt{3}}\right)+m_2\cos\left(e_8+\frac{\varepsilon\sqrt{\frac{2\eta+2c\rho+2\lambda\rho^2}{\rho}}}{\sqrt{3}}\right). \quad (29)$$

By replacing Equation (29) with Equation (5), we obtain

$$\Lambda(\varepsilon) = \frac{12e_3(ie_2+e_4)-2\sqrt{6}m_1\sqrt{\frac{-\eta+\rho(c+\lambda\rho)}{\rho}}\sin(\beta)+2\sqrt{6}\sqrt{c+\frac{\eta}{\rho}+\lambda\rho}\sinh(\varrho)}{3\left(e_2^2+e_4^2+e_9+2ie_2e_3\varepsilon+2e_3e_4\varepsilon+m_1\cos(\beta)+m_2\cosh(\varrho)\right)}. \quad (30)$$

where

$$\beta = e_6+\sqrt{\frac{2}{3}}\varepsilon\sqrt{\frac{-\eta+\rho(c+\lambda\rho)}{\rho}},\ \varrho = e_8+\sqrt{\frac{2}{3}}\varepsilon\sqrt{c+\frac{\eta}{\rho}+\lambda\rho}.$$

Replacing Equation (30) with Equation (2) to find the PCRs of Equation (1) yields

$$\Gamma_5(x,y,t) = \frac{12e_3(ie_2+e_4)-2\sqrt{6}m_1\sqrt{\frac{-\eta+\rho(c+\lambda\rho)}{\rho}}\sin(\phi)+2\sqrt{6}\sqrt{c+\frac{\eta}{\rho}+\lambda\rho}\sinh(\psi)}{3\left(e_2^2+e_4^2+e_9-2ie_2e_3(ct-x+y\rho)-2e_3e_4(ct-x+y\rho)+m_1\cos(\phi)+m_2\cosh(\psi)\right)}. \quad (31)$$

where

$$\phi = e_6+\sqrt{\frac{2}{3}}(ct-x+y\rho)\sqrt{\frac{-\eta+\rho(c+\lambda\rho)}{\rho}},\ \psi = e_8+\sqrt{\frac{2}{3}}(ct-x+y\rho)\sqrt{c+\frac{\eta}{\rho}+\lambda\rho}.$$

7. Multi-Wave Solution

We use the transformation [50]

$$\omega = l_0 \cosh(\varrho) + l_1 \cos(\varrho_1) + l_2 \cos(\varrho_3), \tag{32}$$

where

$$\varrho = m_1\varepsilon + m_2, \;\; \varrho = m_3\varepsilon + m_4, \;\; \varrho_3 = m_5\varepsilon + m_6.$$

However, $m_i (1 \leq i \leq 6)$ are constants. Inserting Equation (32) into Equation (6) yields the following values:

$$m_1 = \sqrt{\tfrac{-(-3\lambda\delta^2 - 3\rho c - 3\eta)}{4\lambda\delta - 3\rho}}, \; m_5 = 0, \; m_3 = \sqrt{\tfrac{-(\lambda\rho^2 + \rho c + \eta)}{2\delta\rho - 2\rho}}. \tag{33}$$

By inserting Equation (33) into Equation (32),we obtain

$$\omega = l_1 \cos(m_4 + \varepsilon\sqrt{\frac{-\eta - c\rho - \lambda\rho^2}{-2\rho + 2\delta\rho}}) + l_2 \cosh(m_6) + l_0 \cosh\left(m_2 + \varepsilon\sqrt{\frac{3\eta + 3c\rho + 3\lambda\rho^2}{-3\rho + 4\delta\rho}}\right). \tag{34}$$

Substituting Equation (34) into Equation (5) yields

$$\Lambda(\varepsilon) = \frac{2(-l_1\varsigma \sin(m_4 + \varepsilon\varsigma + l_0\tau \sinh(m_2 + \varepsilon\tau)))}{l_1 \cos(m_4 + \varepsilon\varsigma) + l_2 \cosh(m_6) + l_0 \cosh(m_2 + \varepsilon\tau)}. \tag{35}$$

where

$$\varsigma = \sqrt{\frac{-\eta - c\rho - \lambda\rho^2}{-2\rho + 2\delta\rho}}, \; \tau = \sqrt{\frac{3\eta + 3c\rho + 3\lambda\rho^2}{-3\rho + 4\delta\rho}}.$$

We then insert Equation (35) into Equation (2) to obtain the multi-wave solution:

$$\Gamma_6(x, y, t) = \frac{2(-l_1\varsigma \sin(m_4 + (-ct + x - y\rho)\varsigma + l_0\tau \sinh(m_2 + (-ct + x - y\rho)\tau)))}{l_1 \cos(m_4 + (-ct + x - y\rho)\varsigma) + l_2 \cosh(m_6) + l_0 \cosh(m_2 + (-ct + x - y\rho)\tau)}. \tag{36}$$

where

$$\varsigma = \sqrt{\frac{-\eta - c\rho - \lambda\rho^2}{-2\rho + 2\delta\rho}}, \; \tau = \sqrt{\frac{3\eta + 3c\rho + 3\lambda\rho^2}{-3\rho + 4\delta\rho}}.$$

8. MSR Interaction with Rogue Waves

We explore the interaction between MSRs and rogue waves using the transformation

$$\omega = o_1^2 + o_2^2 + e^{o_3} + l_0 \cosh(o_4) + p_9, \tag{37}$$

where

$$o_1 = p_1\varepsilon + p_2, \;\; o_2 = p_3\varepsilon + p_4, \;\; o_3 = p_5\varepsilon + p_6.$$

However, $p_i (1 \leq i \leq 9)$ are the parameters. Substituting Equation (37) into Equation (6) yields the values of the assumed parameters:

$$p_1 = \tfrac{-1}{6}\sqrt{2}\sqrt{3}\sqrt{\delta}, \; p_2 = \tfrac{1}{3}\tfrac{\sqrt{2}\sqrt{3}^{\frac{3}{2}}p_5}{(p_5^2 - p_7^2)}, \; p_3 = p_8 = 0, p_9 = \tfrac{-1}{3}\tfrac{(3p_4^2p_5^4 - 6p_4^2p_5^2p_7^2 + 3p_4^2p_7^4 + 2\delta^3p_5^2)}{p_5^4 - 2p_5^2p_7^2 + p_7^4}. \tag{38}$$

Putting Equation (38) in Equation (37) yields

$$\omega = p_4^2 + e^{p_6+p_5\varepsilon} - \left(\frac{(3p_4^2p_5^4 - 6p_4^2p_5^2p_7^2 + 3p_4^2p_7^4 + 2\delta^3p_5^2)}{p_5^4 - 2p_5^2p_7^2 + p_7^4}\right) + \left(\frac{\sqrt{\frac{3}{2}p_5\delta^{\frac{3}{2}}}}{p_5^2 - p_7^2} - \frac{\sqrt{\lambda}}{\sqrt{6}}\right)^2 + l_0\cosh(p_6\varepsilon). \tag{39}$$

By inserting Equation (39) into Equation (5), we obtain

$$\Lambda(\varepsilon) = \frac{2\left(p_5e^{p_6+p_5\varepsilon} - \sqrt{\frac{2}{3}}\sqrt{\delta}\left(\frac{\sqrt{\frac{3}{2}p_5\delta^{\frac{3}{2}}}}{p_5^2-p_7^2} - \frac{\sqrt{\lambda}}{\sqrt{6}}\right) + p_7l_0\sinh(p_7\varepsilon)\right)}{p_4^2 + e^{p_6+p_5\varepsilon} - \left(\frac{(3p_4^2p_5^4-6p_4^2p_5^2p_7^2+3p_4^2p_7^4+2\delta^3p_5^2)}{p_5^4-2p_5^2p_7^2+p_7^4}\right) + \left(\frac{\sqrt{\frac{3}{2}p_5\delta^{\frac{3}{2}}}}{p_5^2-p_7^2} - \frac{\sqrt{\lambda}}{\sqrt{6}}\right)^2 + l_0\cosh(p_6\varepsilon)}. \tag{40}$$

We replace Equation (40) with Equation (2) to find the interaction between the rogue wave and MSR:

$$\Gamma_7(x,y,t) = \frac{2\left(p_5\left(v - \frac{2\delta^2}{p_5^2-p_7^2}\right) + \delta(\phi) + 3p_7l + 0\sinh(p_7(\phi))\right)}{3(p_4^2 + v - \frac{3p_4^2(p_5^2-p_7^2)^2+2p_5^2\delta^3}{3(p_5^2-p_7^2)^2} + \frac{1}{6}\delta\phi^2 + l_0\cosh(\phi))}. \tag{41}$$

where

$$v = e^{p_6+p_5(2p_7^2t+x+\frac{t}{\alpha\delta}\beta-y\rho+t\lambda\rho)},\ \phi = 2p_7^2t + x + \frac{t}{\delta}\beta - y\rho + t\lambda\rho.$$

9. Homoclinic Breather Solutions (HBs)

For HBs, we use [51]

$$\omega = e^{-\mu_1} + m_1e^{\mu_2} + m_2\cos(\mu_3), \tag{42}$$

where

$$\mu_1 = g(n_1\varepsilon + n_2),\ \ \mu_2 = g(n_3\varepsilon + n_4),\ \ \mu_3 = g_1(n_5\varepsilon + n_6).$$

However, $n_i(1 \le i \le 6)$ are all real-valued constants. We use Equation (42) with Equation (6) and evaluate the values of the assumed constants:

$$\delta = \frac{-15}{4},\ n_1 = \frac{\frac{-1}{6}\frac{(\lambda\rho^2+c\rho+\eta)}{\rho}}{g},\ n_3 = 0, n_5 = \frac{\frac{-1}{2}\frac{(-\lambda\rho^2-c\rho-\eta)}{\rho}}{g_1}. \tag{43}$$

Putting Equation (43) into Equation (42) yields

$$\omega = e^{-g(n_2+\frac{\varepsilon\sqrt{\frac{-\eta+c\rho+\lambda\rho^2}{\rho}}}{\sqrt{6}g})} + e^{n_4g}m_1 + m_2\cos\left(g_1\left(n_6 + \frac{\varepsilon\sqrt{\frac{-(-\eta-\rho x-\lambda\rho^2)}{\rho}}}{\sqrt{2}g_1}\right)\right). \tag{44}$$

By inserting Equation (44) into Equation (5), we obtain

$$\Lambda(\varepsilon) = \frac{-\sqrt{6}\sqrt{\frac{-\eta+c\rho+\lambda\rho^2}{\rho}} + 3\sqrt{2}e^{n_2g+\frac{\varepsilon\sqrt{\frac{-\eta+c\rho+\lambda\rho^2}{\rho}}}{\sqrt{6}}}m_2\sqrt{\frac{-\eta+c\rho+\lambda\rho^2}{\rho}}\sin\left(n_6g_1 + \frac{\varepsilon\sqrt{\frac{-\eta+c\rho+\lambda\rho^2}{\rho}}}{\sqrt{2}}\right)}{3\left(1 + e^{n_2g+n_4g+\frac{\varepsilon\sqrt{\frac{-\eta+\rho(c+\lambda\rho)}{\rho}}}{\sqrt{6}}}m_1 + e^{n_2g+\frac{\varepsilon\sqrt{\frac{-\eta+\rho(c+\lambda\rho)}{\rho}}}{\sqrt{6}}}m_2\cos\left(n_6g_1 + \frac{\varepsilon\sqrt{\frac{-\eta+\rho(c+\lambda\rho)}{\rho}}}{\sqrt{2}}\right)\right)}. \tag{45}$$

We then substitute Equation (45) into Equation (2) to find the HBs:

$$\Gamma_8(x,y,t) = \frac{-\sqrt{6}\sqrt{\frac{-\eta+c\rho+\lambda\rho^2}{\rho}} + 3\sqrt{2}\varphi m_2\sqrt{\frac{-\eta+c\rho+\lambda\rho^2}{\rho}}\sin(\phi)}{3(1+e^{n_2 g+n_4 g+\frac{(-ct+x-\rho y)\sqrt{\frac{-\eta+\rho(c+\lambda\rho)}{\rho}}}{\sqrt{6}}}m_1+\varphi m_2\cos(\phi))}, \tag{46}$$

where

$$\phi = n_6 g_1 + \frac{(-ct+x-\rho y)\sqrt{\frac{-\eta+c\rho+\lambda\rho^2}{\rho}}}{\sqrt{2}},\ \varphi = e^{n_2 g+\frac{(-ct+x-\rho y)\sqrt{\frac{-\eta+c\rho+\lambda\rho^2}{\rho}}}{\sqrt{6}}}.$$

10. Stability Property of Solutions

Now, using a Hamiltonian approach, we will examine the stability property for a $(2+1)$-dimensional KdV equation of constant coefficients. The Hamiltonian methodology "K" is given by

$$K = \frac{1}{2}\int_{-h}^{h} \Upsilon^2(z)dz. \tag{47}$$

The solutions' stability condition can be assessed as follows:

$$\frac{\partial K}{\partial \rho} > 0. \tag{48}$$

The wave velocity is ρ, and K stands for the momentum in the Hamiltonian system. Using the Hamiltonian system, the stability's condition is stated, and all feasible solutions are then determined (Table 1).

Table 1. Stability properties of the solutions $\Gamma_i(x,y,t)$, where $(i = 1,2,3,...,8)$.

Solution	Stable	Unstable	Values of Variables
$\Gamma_1(x,y,t)$	✓		$\eta=-1,\ c=2,\ \rho=2,\ \lambda=2,\ m_4=9,\ x,y,t\in[-7,7]$
$\Gamma_2(x,y,t)$	✓		$g_6=8,\ c=1,\ \rho=-1,\ \eta=1,\ \lambda=1,\ g_1=3,$ $\delta=3,\ g_4=2,\ z_1=1,\ t=5,\ x,y,t\in[-1,1]$
$\Gamma_3(x,y,t)$	✓		$c=1.7,\ \rho=4,\ z_1=3,\ u_8=2,\ \eta=2,\ u_3=-1,$ $z_2=1,\ \delta=2,\ \lambda=2,\ t=1,\ u_6=9,\ x,y,t\in[-2,2]$
$\Gamma_4(x,y,t)$		✓	Singular solution
$\Gamma_5(x,y,t)$		✓	Singular solution
$\Gamma_6(x,y,t)$	✓		$l_1=4,\ \eta=1,\ c=1,\ \rho=3,\ l_0=2,\ m_2=3,\ m_6=2,$ $\lambda=1.2,\ \delta=2,\ l_2=12,\ t=9,\ m_4=3,\ x,y,t\in[-3,3]$
$\Gamma_7(x,y,t)$	✓		$p_6=3.3,\ p_5=1,\ p_7=1.2,\ \delta=1.5,\ l_0=2,\ \eta=3,$ $\rho=2,\ \lambda=2,\ p_4=1,\ t=-1,\ x,y,t\in[-11,11]$
$\Gamma_8(x,y,t)$		✓	Singular solution

11. Results and Discussion

With the help of the proper parameter settings, we were able to successfully produce the desired type of solution, which illustrates a wave discrepancy. In Figure 1, the wave appears in the MSRs with $\eta = -1$, $c = 2$, $\rho = 2$, $\lambda = 2$, $m_4 = 9$, and $t = 11$. We can see how the wave moves and changes its position with various values for the time parameter t. Figures 2 and 3 display the movement of the wave and the stability conditions with $t = 9$ and $t = -6$, respectively. In Figure 4, we explore MSRs with exponential functions with 3D, contour, 2D, and stream plots via $g_6 = 8$, $c = 1$, $\rho = -1$, $\eta = 1$, $\lambda = 1$, $g_1 = 3$, $\delta = 3$, $g_4 = 2$, $z_1 = 1$, and $t = 5$. Figures 5 and 6 show a wave with a high amplitude. Figure 7 shows the interaction solution between the MSRs and kink

II via 3D, 2D, contour, and stream plots with $c = 1.7$, $\rho = 4$, $z_1 = 3$, $u_8 = 2$, $\eta = 2$, $u_3 = -1$, $z_2 = 1$, $\delta = 2$, $\lambda = 2$, $t = 1$, and $u_6 = 9$. In Figure 8, various bright and dark lumps appear via the assumed parameters $c = 1.7$, $\rho = 4$, $z_1 = 3$, $u_8 = 2$, $\eta = 2$, $u_3 = -1$, $z_2 = 1$, $\delta = 2$, $\lambda = 2$, $t = 1$, and $u_6 = 3$. Figure 9 depicts PKCs in which a soliton wave appears with a high amplitude via $g_3 = 6$, $c = 1$, $\rho = 2$, $g_5 = 3$, $\eta = 1$, $\lambda = 1$, $g_2 = 5$, $m_0 = 5$, $g_7 = 11$, and $t = 3$.

The PKCs in Equation (31) are graphically presented in Figures 10 and 11. Figure 12 shows a visual representation of the multi-wave solution in Equation (36) in which multiple bright lumps appear, considering $l_1 = 4$, $\eta = 1$, $c = 1$, $\rho = 3$, $l_0 = 2$, $m_2 = 3$, $m_6 = 2$, $\lambda = 1.2$, $\delta = 2$, $l_2 = 12$, $t = 9$, and $m_4 = 3$. The multi-wave shape profiles are explained via $l_1 = 4$, $\eta = 1$, $c = 1$, $\rho = 3$, $l_0 = 2$, $m_2 = 3$, $m_6 = 2$, $\lambda = 1.2$, $\delta = 2$, $l_2 = 12$, $t = 9$, and $m_4 = 2.5$ in Figure 13. For various parametric values, we attained the multi-wave sketches in Figure 14 via $l_1 = 4$, $\eta = 1$, $c = 1$, $\rho = 3$, $l_0 = 2$, $m_2 = 3$, $m_6 = 2$, $\lambda = 1.2$, $\delta = 2$, $l_2 = 12$, $t = 9$, and $m_4 = 4.5$. In Figure 15, we constructed the interactional solution between the MSRs and rogue wave profiles via $p_6 = 3.3$, $p_5 = 1$, $p_7 = 1.2$, $\delta = 1.5$, $l_0 = 2$, $\eta = 3$, $\rho = 2$, $\lambda = 2$, $p_4 = 1$, and $t = -1$. The dynamical behavior of the solution in Equation (41) via $p_6 = 3.3$, $p_5 = 1$, $p_7 = 1.2$, $\delta = 1.5$, $l_0 = 2$, $\eta = 3$, $\rho = 2$, $\lambda = 2$, $p_4 = 1$, and $t = 3$ is presented in Figure 16. With $p_6 = 3.3$, $p_5 = 1$, $p_7 = 1.2$, $\delta = 1.5$, $l_0 = 2$, $\eta = 3$, $\rho = 2$, $\lambda = 2$, $p_4 = 1$, and $t = 5$, the solution to the MSRs with rogue waves via three-dimensional, contour, two-dimensional, and stream plots are shown in Figure 17. We attained HBs using Equation (46) with $\eta = 2$, $\rho = 1.3$, $c = 3.1$, $\lambda = -2$, $n_2 = -2$, $n_6 = 3$, $m_2 = -1$, $m_1 = 2$, $m_4 = 3$, $g_1 = -5$, and $t = 3$. Figure 18 shows 3D visuals of the homoclinic solution with (1) Figure 18a with $g = -0.4$, (2) Figure 18b with $g = -1.4$, (3) Figure 18c with $g = -2.4$, and (4) Figure 18d with $g = -4.4$. Figure 19 shows the stability conditions corresponding to Figure 18.

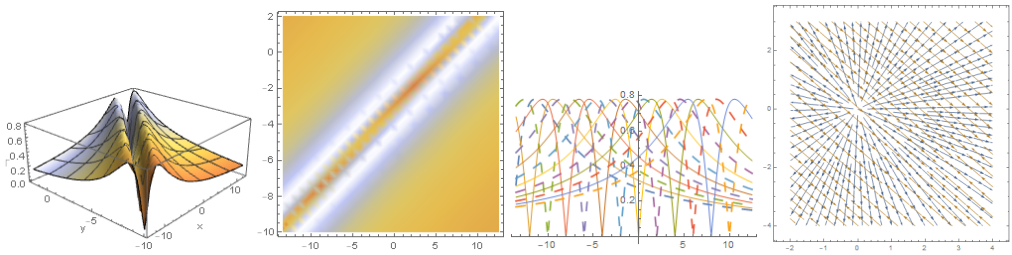

Figure 1. Evolution plots for $\Gamma_1(x, y, t)$ with the values $\eta = -1$, $c = 2$, $\rho = 2$, $\lambda = 2$, $m_4 = 9$, and $t = 11$.

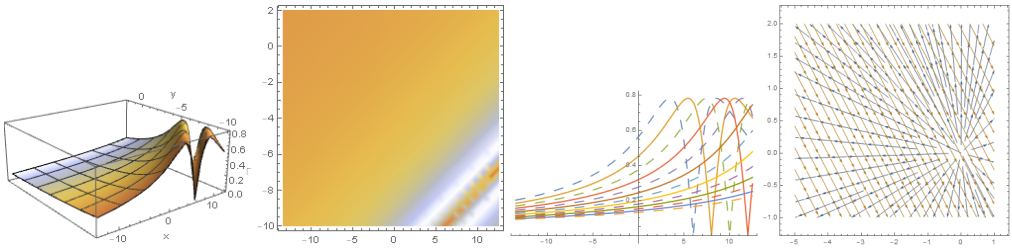

Figure 2. MSR graphic profiles for $\Gamma_1(x, y, t)$ with $t = 9$.

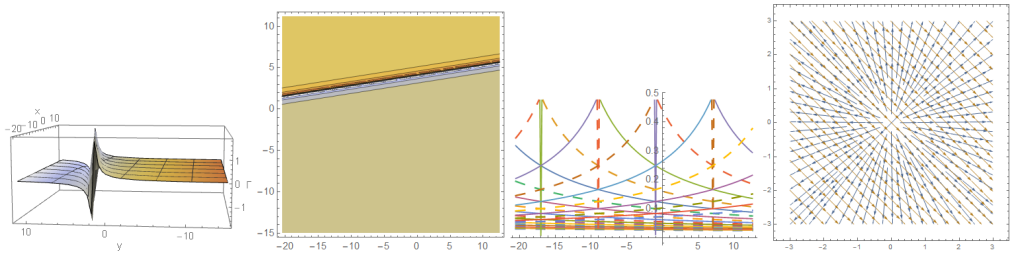

Figure 3. MSR visual representation for $\Gamma_1(x, y, t)$ with $t = -6$.

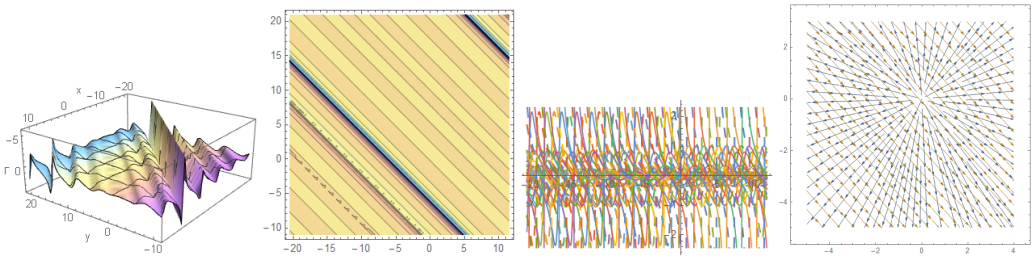

Figure 4. The dynamical behavior of MSR with one exponential function solution via $g_6 = 8$, $c = 1$, $\rho = -1$, $\eta = 1$, $\lambda = 1$, $g_1 = 3$, $\delta = 3$, $g_4 = 2$, $z_1 = 1$, and $t = 5$.

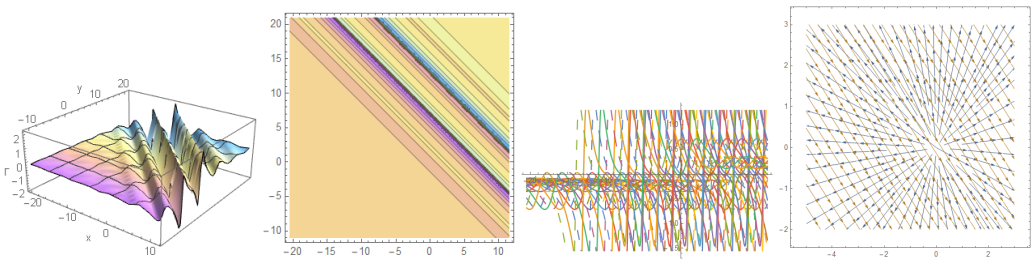

Figure 5. The plots of $\Gamma_2(x, y, t)$ via $g_6 = 5$, $c = 1$, $\rho = -1$, $\eta = 1$, $\lambda = 1$, $g_1 = 3$, $\delta = -2$, $g_4 = 3$, $z_1 = 1$, and $t = 5$.

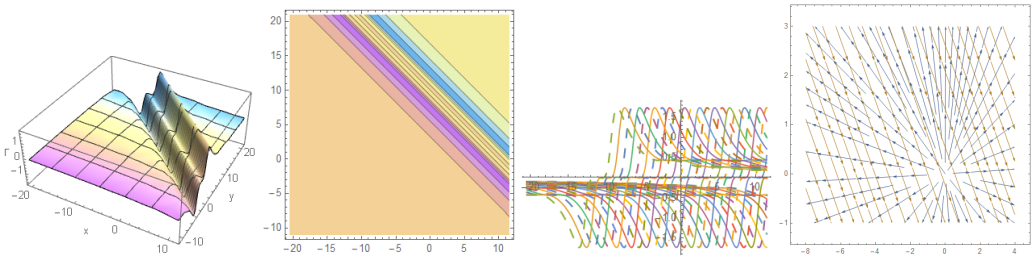

Figure 6. The graphs of $\Gamma_2(x, y, t)$ in Equation (16) via $g_6 = 3$, $c = 1$, $\rho = -1$, $\eta = 1$, $\lambda = 1$, $g_1 = 3$, $\delta = -2$, $g_4 = 3$, $z_1 = 1$, and $t = 5$.

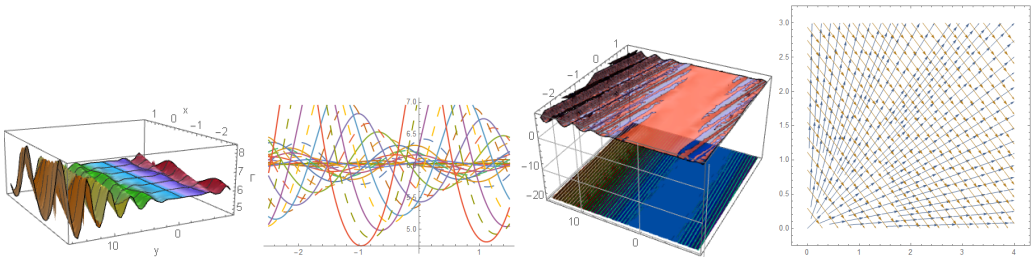

Figure 7. The graphical profiles of MSR with double exponential function along with $c = 1.7$, $\rho = 4$, $z_1 = 3$, $u_8 = 2$, $\eta = 2$, $u_3 = -1$, $z_2 = 1$, $\delta = 2$, $\lambda = 2$, $t = 1$, and $u_6 = 9$.

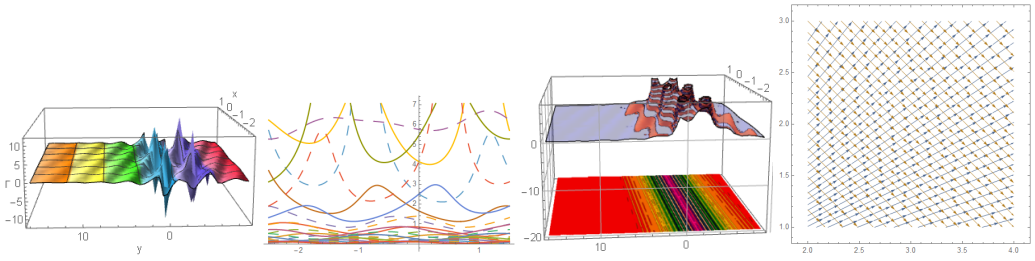

Figure 8. The dynamical behavior of M-shaped funciton with two kinks via $c = 1.7$, $\rho = 4$, $z_1 = 3$, $u_8 = 2$, $\eta = 2$, $u_3 = -1$, $z_2 = 1$, $\delta = 2$, $\lambda = 2$, $t = 1$, and $u_6 = 3$.

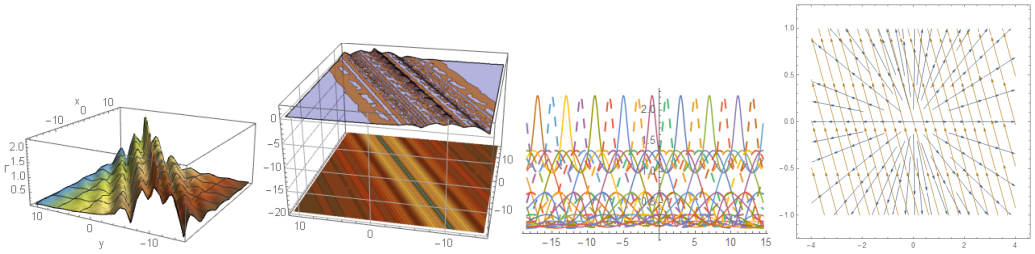

Figure 9. The sketch of $\Gamma_4(x,y,t)$ in Equation (31) via $q_3 = 6$, $c = 1$, $e_4 = 4$, $\rho = 2$, $q_5 = 3$, $\eta = 1$, $q_2 = 5$, $\lambda = 1$, $q_7 = 11$, $m_0 = 5$, and $t = 3$.

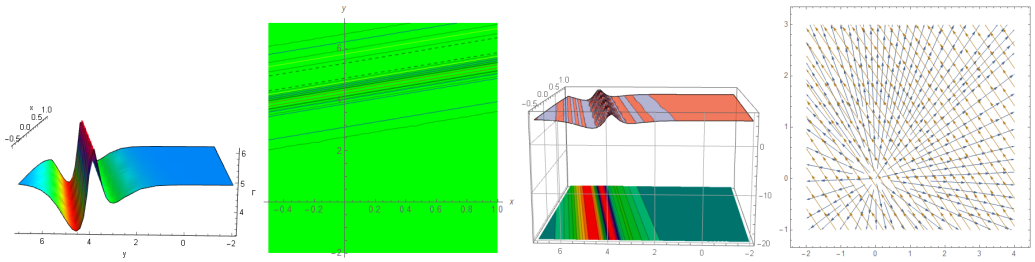

Figure 10. The pictorial representation of PCRs in Equation (31) with $e_3 = 11$, $e_2 = 4.9$, $e_4 = 4$, $m_1 = 14$, $e_6 = 5$, $\eta = 1$, $c = 2$, $\lambda = 6$, $e_9 = 3.1$, $m_2 = 8.5$, $e_8 = 3$, $t = -2$, and $\rho = 1$.

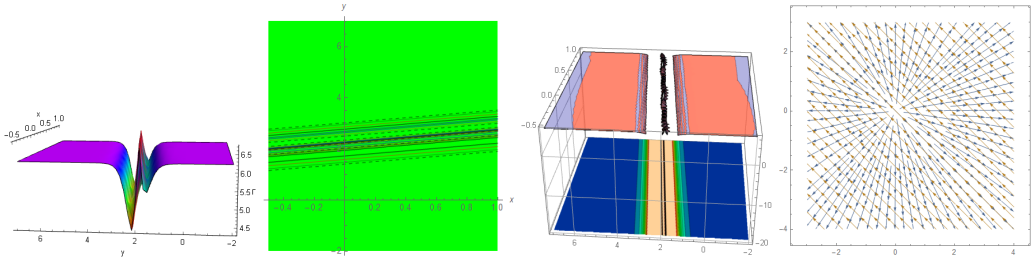

Figure 11. The sketch of $\Gamma_5(x,y,t)$ in Equation (31) via $e_3 = 11$, $e_2 = 4.9$, $e_4 = 4$, $m_1 = 14$, $e_6 = 5$, $\eta = 1$, $c = 2$, $\lambda = 6$, $e_9 = 3.1$, $m_2 = 8.5$, $e_8 = 3$, $t = -2$, and $\rho = 1$.

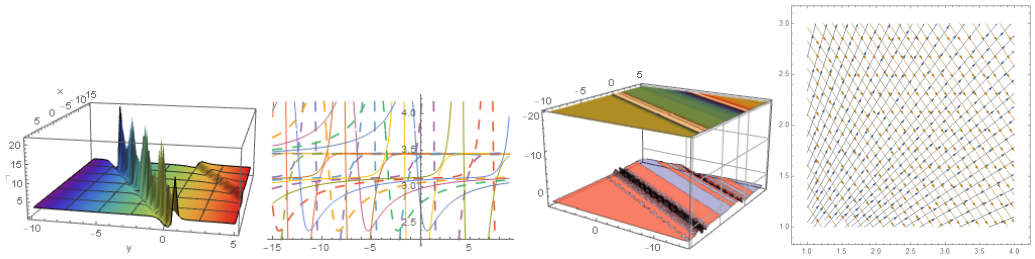

Figure 12. Multi-wave shape profiles of $\Gamma_6(x,ty,t)$ in Equation (36) via $l_1 = 4$, $\eta = 1$, $c = 1$, $\rho = 3$, $l_0 = 2$, $m_2 = 3$, $m_6 = 2$, $\lambda = 1.2$, $\delta = 2$, $l_2 = 12$, $t = 9$, and $m_4 = 3$.

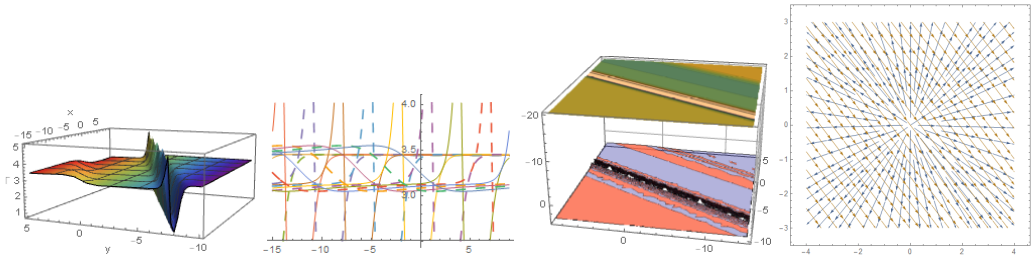

Figure 13. Multi-wave dynamical behavior via $l_1 = 4$, $\eta = 1$, $c = 1$, $\rho = 3$, $l_0 = 2$, $m_2 = 3$, $m_6 = 2$, $\lambda = 1.2$, $\delta = 2$, $l_2 = 12$, $t = 9$, and $m_4 = 2.5$.

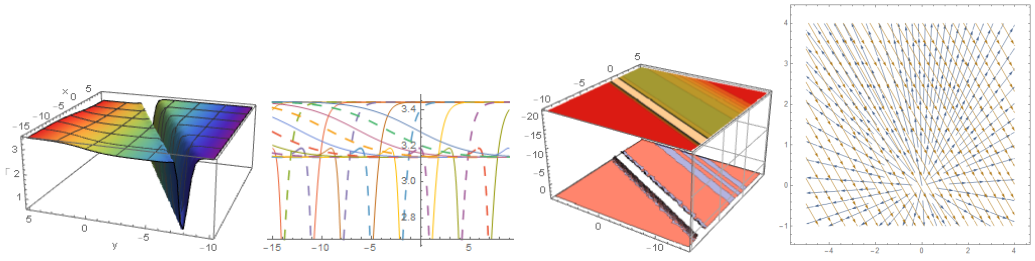

Figure 14. Multi-wave sketches of $\Gamma_6(x, ty, t)$ in Equation (36) via $l_1 = 4$, $\eta = 1$, $c = 1$, $\rho = 3$, $l_0 = 2$, $m_2 = 3$, $m_6 = 2$, $\lambda = 1.2$, $\delta = 2$, $l_2 = 12$, $t = 9$, and $m_4 = 4.5$.

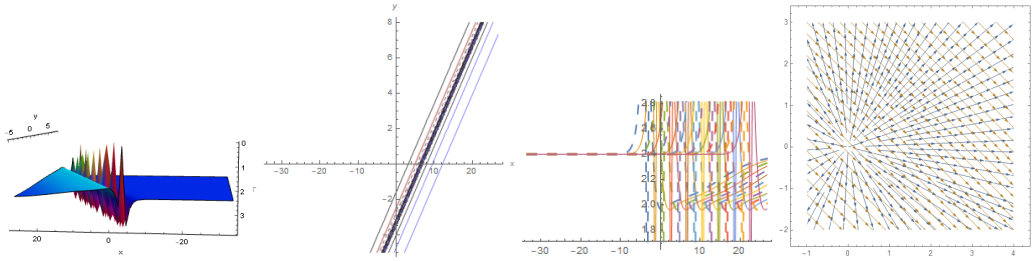

Figure 15. $\Gamma_7(x, y, t)$ in Equation (41) is plotted with $p_6 = 3.3$, $p_5 = 1$, $p_7 = 1.2$, $\delta = 1.5$, $l_0 = 2$, $\eta = 3$, $\rho = 2$, $\lambda = 2$, $p_4 = 1$, and $t = -1$.

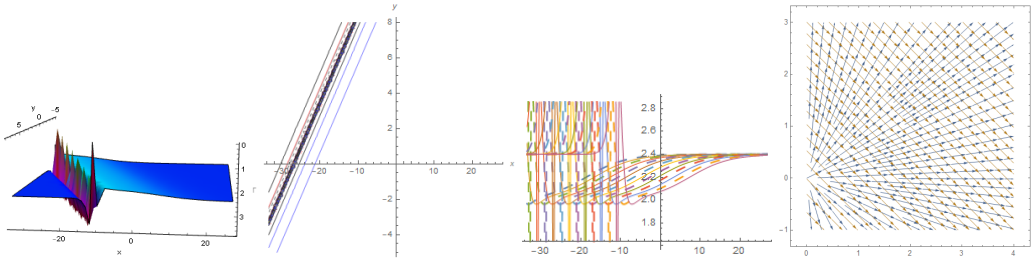

Figure 16. Interaction solution in Equation (41) presented graphically with $p_6 = 3.3$, $p_5 = 1$, $p_7 = 1.2$, $\delta = 1.5$, $l_0 = 2$, $\eta = 3$, $\rho = 2$, $\lambda = 2$, $p_4 = 1$, and $t = 3$.

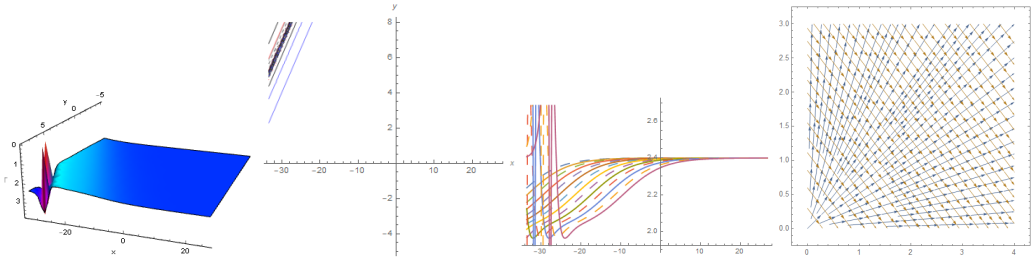

Figure 17. $\Gamma_7(x, y, t)$ in Equation (41) sketched via $p_6 = 3.3$, $p_5 = 1$, $p_7 = 1.2$, $\delta = 1.5$, $l_0 = 2$, $\eta = 3$, $\rho = 2$, $\lambda = 2$, $p_4 = 1$, and $t = 5$.

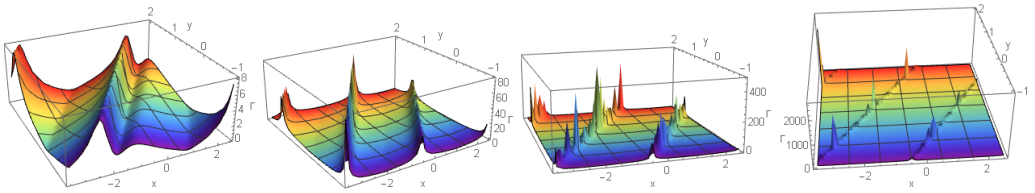

(**a**) $g = -0.4$ (**b**) $g = -1.4$ (**c**) $g = -2.4$ (**d**) $g = -4.4$

Figure 18. The 3D HB profiles for $\Gamma_8(x, y, t)$ with $\eta = 2$, $\rho = 1.3$, $c = 3.1$, $\lambda = -2$, $n_2 = -2$, $n_6 = 3$, $m_2 = -1$, $m_1 = 2$, $m_4 = 3$, $g_1 = -5$, and $t = 3$.

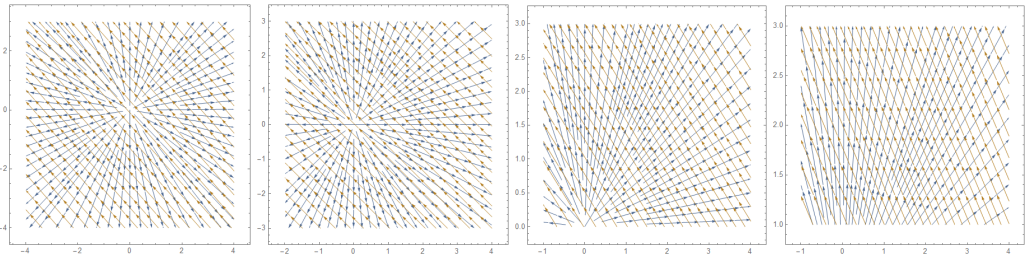

(**a**) $g = -0.4$ (**b**) $g = -1.4$ (**c**) $g = -2.4$ (**d**) $g = -2.4$

Figure 19. Stream plots corresponding to Figure 18.

12. Conclusions

Some analytical solutions were acquired by symbolic computations. Additionally, a thorough investigation of the solutions' dynamics was conducted. In this work, the MSRs, multi-wave solitons, RKCs, PCRs, HBs, and interactional solutions such as MSRs with one kink, double kinks, and rogue waves were all studied. Using the Hamilton system features, we identified solutions as stable or unstable solutions. Finally, the findings were graphically analyzed using contour, density, three-dimensional, two-dimensional, and stream plots. We obtained entirely unique outcomes with our research.

Author Contributions: Conceptualization, S.T.R.R.; Methodology, S.T.R.R.; Writing—review & editing, H.Z.; Supervision, A.R.S. All authors have read and agreed to the published version of the manuscript.

Funding: Deputyship for Research and Innovation of the Ministry of Education in Saudi Arabia for funding this research work (project number 141/442).

Data Availability Statement: Not applicable.

Acknowledgments: The authors extend their appreciation to the Deputyship for Research and Innovation of the Ministry of Education in Saudi Arabia for funding this research work (project number 141/442). Additionally, the authors would like to extend their appreciation to Taibah University for its supervision support.

Conflicts of Interest: The authors declare no conflict of interest.

References

1. Batool, T.; Rizvi, S.T.R.; Seadawy, A.R. Multiple breathers and rational solutions to Ito integro-differential equation arising in shallow water waves. *J. Geom. Phys.* **2022**, *178*, 104540. [CrossRef]
2. Rizvi, S.T.R.; Seadawy, A.R.; Batool, T.; Ashraf, M.A. Homoclinic breaters, mulitwave, periodic cross-kink and periodic cross-rational solutions for improved perturbed nonlinear Schrödinger's with quadratic-cubic nonlinearity. *Chaos Solitons Fractals* **2022**, *161*, 112353. [CrossRef]
3. Rizvi, S.T.R.; Seadawy, A.R.; Raza, U. Detailed analysis for chirped pulses to cubic-quintic nonlinear non-paraxial pulse propagation model. *J. Geom. Phys.* **2022**, *178*, 104561. [CrossRef]
4. Rizvi, S.T.R.; Seadawy, A.R.; Farrah, N.; Ahmad, S. Application of Hirota operators for controlling soliton interactions for Bose-Einstien condensate and quintic derivative nonlinear Schrödinger equation. *Chaos Solitons Fractals* **2022**, *159*, 112128. [CrossRef]
5. Rizvi, S.T.R.; Seadawy, A.R.; Ahmed, S.; Younis, M.; Ali, K. Study of multiple lump and rogue waves to the generalized unstable space time fractional nonlinear Schrödinger equation. *Chaos Solitons Fractals* **2021**, *151*, 111251. [CrossRef]
6. Ali, K.; Seadawy, A.R.; Ahmad, S.; Rizvi, S.T.R. Discussion on rational solutions for Nematicons in liquid crystal with Kerr law. *Chaos Solitons Fractals* **2022**, *160*, 112218. [CrossRef]
7. Seadawy, A.R.; Ahmad, S.; Rizvi, S.T.R.; Ali, K. Various forms of lumps and interaction solutions to generalized Vakhnenko Parkes equation arising from high-frequency wave propagation in electromagnetic physics. *J. Geom. Phys.* **2022**, *176*, 104507. [CrossRef]
8. Seadawy, A.R.; Younis, M.; Baber, M.Z.; Iqbal, M.S.; Rizvi, S.T.R. Nonlinear acoustic wave structures to the Zabolotskaya Khokholov dynamical model. *J. Geom. Phys.* **2022**, *175*, 104474. [CrossRef]
9. Seadawy, A.R.; Rizvi, S.T.R.; Mustafa, B.; Ali, K.; Althubiti, S. Chirped periodic waves for an cubic quintic nonlinear Schrödinger equation with self steepening and higher order nonlinearities. *Chaos Solitons Fractals* **2022**, *156*, 111804. [CrossRef]

10. Seadawy, A.R.; Bilal, M.; Younis, M.; Rizvi, S.T.R.; Althobaiti, S.; Makhlouf, M.M. Analytical mathematical approaches for the double chain model of DNA by a novel computational technique. *Chaos Solitons Fractals* **2021**, *144*, 110669. [CrossRef]
11. Inan, I.E. Multiple Soliton Solutions of Some Nonlinear Partial Differential Equations. *Univers. J. Math. Appl.* **2018**, *1*, 273–279. [CrossRef]
12. Dubard, P.; Gaillard, P.; Klein, C.; Matveev, V.B. On multi-rogue wave solutions of the NLS equation and positon solutions of the KdV equation. *Eur. Phys. J. Spec. Top.* **2010**, *185*, 247–258. [CrossRef]
13. Bock, T.L.; Kruskal, M.D. A two-parameter Miura transformation of the Benjamin-Ono equation. *Phys. Lett. A* **1979**, *74*, 173–176. [CrossRef]
14. Abourabia, A.M.; El Horbaty, M.M. On solitary wave solutions for the two-dimensional nonlinear modified Kortweg-de Vries-Burger equation. *Chaos Solitons Fractals* **2006**, *29*, 354–364. [CrossRef]
15. Malfliet, W. Solitary wave solutions of nonlinear wave equations. *Am. J. Phys.* **1992**, *60*, 650. [CrossRef]
16. Taghizadeh, N.; Mirzazadeh, M.; Farahrooz, F. Exact solutions of the nonlinear Schrödinger equation by the first integral method. *J. Math. Anal. Appl.* **2011**, *374*, 549–553. [CrossRef]
17. Elwakil, S.A.; El-labany, S.K.; Zahran, M.A.; Sabry, R. Modified extended tanh-function method for solving nonlinear partial differential equations. *Phys. Lett. A* **2002**, *299*, 179–188. [CrossRef]
18. Chen, H.; Zhang, H. New multiple soliton solutions to the general Burgers-Fisher equation and the Kuramoto-Sivashinsky equation. *Chaos Solitons Fractals* **2004**, *19*, 71–76. [CrossRef]
19. Liu, S.; Fu, Z.; Liu, S.; Zhao, Q. Jacobi elliptic function expansion method and periodic wave solutions of nonlinear wave equations. *Phys. Lett. A* **2001**, *289*, 69–74. [CrossRef]
20. Shen, S.; Yang, Z.; Li, X.; Zhang, S. Periodic propagation of complex-valued hyperbolic-cosine-Gaussian solitons and breathers with complicated light field structure in strongly nonlocal nonlinear media. *Commun. Nonlinear Sci. Numer. Simul.* **2021**, *103*, 106005. [CrossRef]
21. Shen, S.; Yang, Z.; Pang, Z.-G.; Ge, Y.-R. The complex-valued astigmatic cosine-Gaussian soliton solution of the nonlocal nonlinear Schrödinger equation and its transmission characteristics. *Appl. Math. Lett.* **2022**, *125*, 107755. [CrossRef]
22. Song, L.-M.; Yang, Z.; Li, X.-L.; Zhang, S.-M. Coherent superposition propagation of Laguerre–Gaussian and Hermite–Gaussian solitons. *Appl. Math. Lett.* **2020**, *102*, 106114. [CrossRef]
23. Marin, M.; Othman, M.I.A.; Seadawy, A.R.; Carstea, C. A domain of influence in the Moore–Gibson–Thompson theory of dipolar bodies. *J. Taibah Univ. Sci.* **2020**, *14*, 653–660. [CrossRef]
24. Marin, M.; Seadawy, A.; Vlase, S.; Chirila, A. On mixed problem in thermoelasticity of type III for Cosserat media. *J. Taibah Univ. Sci.* **2022**, *16*, 1264–1274. [CrossRef]
25. Darvishi M.T.; Najafi M.; Kavitha L.; Venkatesh M. Stair and Step Soliton Solutions of the Integrable (2+1) and (3+1)-Dimensional Boiti—Leon—Manna—Pempinelli Equations. *Commun. Theor. Phys.* **2012**, *58*, 785. [CrossRef]
26. Darvishi, M.T.; Kavitha, L.; Najafi, M.; Senthil Kumar, V. Elastic collision of mobile solitons of a (3+1)-dimensional soliton equation. *Nonlinear Dyn.* **2016**, *86*, 765–778. [CrossRef]
27. Huai-Tang, C.; Hong-Qing, Z. New double periodic and multiple soliton solutions of the generalized (2+1)-dimensional Boussinesq equation. *Chaos Solitons Fractals* **2004**, *20*, 765–769. [CrossRef]
28. Chen, Y.; Wang, Q.; Lic, B. Jacobi Elliptic Function Rational Expansion Method with Symbolic Computation to Construct New Doubly-periodic Solutions of Nonlinear Evolution Equations. *Z. für Naturforschung A* **2004**, *59*, 529–536. [CrossRef]
29. Chen, Y.; Yan, Z. The Weierstrass elliptic function expansion method and its applications in nonlinear wave equations. *Chaos Solitons Fractals* **2006**, *29*, 948–964. [CrossRef]
30. Wang, M.; Li, X.; Zhang, J. The $(\frac{G'}{G})$-expansion method and travelling wave solutions of nonlinear evolution equations in mathematical physics. *Phys. Lett. A* **2008**, *372*, 417–423. [CrossRef]
31. Lu, H.; Li, X.; Niu, L. A generalized expansion method and its applications to nonlinear evolution equations. *Appl. Math. Comput.* **2010**, *215*, 3811–3816.
32. Ablowitz, M.J.; Clarkson, P.A. *Solitons, Nonlinear Evolution Equations and Inverse Scattering Transform*; Cambridge University Press: Cambridge, UK, 1991.
33. Dong, H.; Wei, C.; Zhang, Y.; Liu, M.; Fang, Y. The Darboux Transformation and N-Soliton Solutions of Coupled Cubic-Quintic Nonlinear Schrödinger Equation on a Time-Space Scale. *Fractal Fract.* **2022**, *6*, 12. [CrossRef]
34. Ebaid, A.; Aly, E.H. Exact solutions for the transformed reduced Ostrovsky equation via the F-expansion method in terms of Weierstrass-elliptic and Jacobian-elliptic functions. *Wave Motion* **2012**, *49*, 296–308. [CrossRef]
35. Li, B.; Chen, Y. Nonlinear Partial Differential Equations Solved by Projective Riccati Equations Ansatz. *Z. Naturforschung A* **2003**, *58a*, 511–519. [CrossRef]
36. Cariello, F.; Tabor, M. Similarity reductions from extended Painleve expansions for nonintegrable evolution equations. *Phys. D Nonlinear Phenom.* **1991**, *53*, 59–70. [CrossRef]
37. Wu, H.Y. On Bäcklund Transformations for Nonlinear Partial Differential Equations. *J. Math. Anal. Appl.* **1995**, *192*, 151–179. [CrossRef]
38. He, J.-H.; Wu, X.-H. Exp-function method for nonlinear wave equations. *Chaos Solitons Fractals* **2006**, *30*, 700–708. [CrossRef]
39. Fan, E. Extended tanh-function method and its applications to nonlinear equations. *Phys. Lett. A* **2000**, *277*, 212–218. [CrossRef]

40. Evans, D.J.; Raslan, K.R. The tanh function method for solving some important non-linear partial differential equations. *Int. J. Comput. Math.* **2004**, *82*, 897–905. [CrossRef]
41. Naher, H.; Abdullah, F. New generalized and improved (G′/G)-expansion method for nonlinear evolution equations in mathematical physics. *J. Egypt. Math. Soc.* **2014**, *22*, 390–395. [CrossRef]
42. Wazwaz, A.-M. Two new Painleve-integrable (2+1) and (3+1)-dimensional KdV equations with constant and time-dependent coefficients. *Nucl. Phys. B* **2020**, *954*, 115009. [CrossRef]
43. Ma, W.-X. N-soliton solutions and the Hirota conditions in (2+1)-dimensions. *Opt. Quantum Electron.* **2020**, *52*, 511. [CrossRef]
44. Ma, W.-X.; Yong, X.; Zhang, H.-Q. Diversity of interaction solutions to the (2+1)-dimensional Ito equation. *Comput. Math. Appl.* **2018**, *75*, 289–295. [CrossRef]
45. Zayed, E.M.E.; Abdelaziz, M.A.M. The Two Variable $(\frac{G'}{G}, \frac{1}{G})$-Expansion Method for Solving the Nonlinear KdV-mKdV Equation. *Math. Probl. Eng.* **2012**, *2012*, 725061. [CrossRef]
46. Yang, J.Y.; Ma, W.X.; Qin, Z. Lump and lump-soliton solutions to the (2+1)-dimensional Ito equation. *Anal. Math. Phys.* **2018**, *8*, 427–436. [CrossRef]
47. Rizvi, S.T.R.; Seadawy, A.R.; Ashraf, M.A.; Younis, M.; Khaliq, A.; Baleanu, D. Rogue, multi-wave, homoclinic breather, *M*-shaped rational and periodic-kink solutions for a nonlinear model describing vibrations. *Results Phys.* **2021**, *29*, 104654. [CrossRef]
48. Ahmed, I.; Seadawy, A.R.; Lu, D. *M*-shaped rational solitons and their interaction with kink waves in the Fokas-lenells equation. *Phys. Scr.* **2019**, *94*, 055205. [CrossRef]
49. Ma, H.; Zhang, C.; Deng, A. New periodic wave, cross-kink wave, breather, and the interaction phenomenon for the (2+1)-dimensional Sharmo-Tasso-Olver equation. *Complexity* **2020**, *2020*, 4270906. [CrossRef]
50. Ahmed, I.; Seadawy, A.R.; Lu, D. Kinky breathers, *W*-shaped and multi-peak solitons interaction in (2+1)-dimensional nonlinear Schrödinger equation with Kerr law of nonlinearity. *Eur. Phys. J. Plus* **2019**, *134*, 120. [CrossRef]
51. Seadawy A.R. Stability analysis for Zakharov-Kuznetsov equation of weakly nonlinear ion-acoustic waves in a plasma. *Comput. Math. Appl.* **2014**, *67*, 172–180. [CrossRef]